A Framework for Mitigating the Biases in Barometric Dust Devil Surveys

Brian Jackson[1] (bjackson@boisestate.edu) and Ralph Lorenz[2], [1]Boise State University, 1910 University Drive, Boise ID 83725-1570, [2]Applied Physics Laboratory, The Johns Hopkins University, Laurel, Maryland

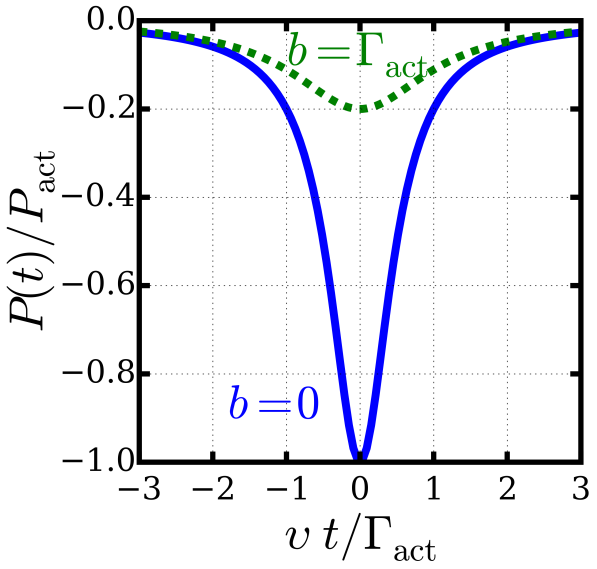

Figure 1: Dust devil profiles $P(t)$ measured in time t for a closest approach distance $b = 0$ and $b = \Gamma_{\rm act}$, i.e. for a closest approach equal to the profile's diameter.

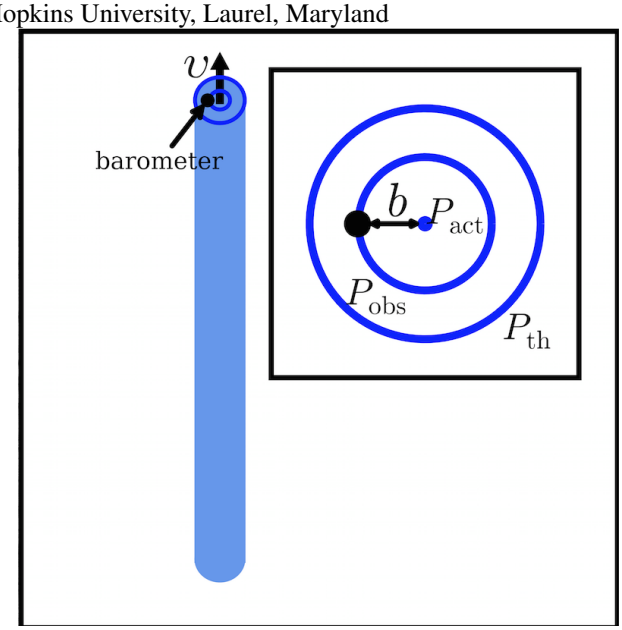

Figure 2: Geometry of dust devil encounter. The blue circles show pressure contours. The pressure signal recorded is $P_{\rm obs}$ and must be exceed the threshold pressure for detection $P_{\rm th}$. The shaded blue region shows the area of the surface carved out by this threshold pressure contour.

Introduction: Dust devils are few to many tens of meter, low-pressure vortices lofting dust, and they occur ubiquitously on Mars, where they may dominate the supply of atmospheric dust and influence climate [1]. The dust-lifting capacity of dust devils depends sensitively on the pressure wells at their centers [2], so the dust supply on Mars may be dominated by the seldom-observed larger devils. Thus, elucidating the origin, evolution, and population statistics of dust devils is critical for understanding Martian atmospheric properties.

Studies of Martian dust devils have been conducted using pressure time-series from in-situ meteorological instrumentation [3]. Recently, similar terrestrial surveys have been conducted using in-situ single barometers [4, 5, 6]. For these surveys, a dust devil passing nearby will register as a dip in the pressure time-series - Figure 1.

As cost-effective as they are, such surveys suffer important biases. In particular, a fixed barometric sensor is more likely to have a more distant encounter with a dust devil. Since a devil's pressure profile falls off with distance, the deepest point in the observed profile will almost always be less than the actual pressure well at the devil's center. Simple geometric considerations can mitigate the influence of this miss distance effect, though, providing more accurate estimates of the population statistics.

De-Biasing the Observed Dust Devil Population: The geometry of encounter between the pressure sensor and dust devil is shown in Figure 2. For our model, we make several assumptions, including: (1) each dust devil pressure profile has a well-defined, static Lorentzian profile with a central pressure $P_{\rm act}$ and width $\Gamma_{\rm act}$ that falls off with radial distance r; and (2) the dust devil center travels at a constant velocity υ.

We can relate the geometry of an encounter directly to the observed profile parameters. As a devil passes the barometer, $r(t) = \sqrt{b^2 + (\upsilon t)^2}$, where time t runs from negative to positive values.

The deepest point observed in the pressure profile $P_{\rm obs}$ is given by

$$P_{\rm obs} = P_{\rm act} / \left(1 + (2b/\Gamma_{\rm act})^2\right). \quad (1)$$

Clearly, unless $b = 0$, $P_{\rm obs} < P_{\rm act}$. Likewise, non-central encounters will distort the profile full-width/half-max, giving a full-width/half-max $\Gamma_{\rm obs}$, which is given by

$$\Gamma_{\rm obs}^2 = \Gamma_{\rm act}^2 + (2b)^2 \,. \tag{2}$$

The probability density for passing between b and $b + db$ of a devil is $dp(b) = 2b\ db/b_{\rm max}^2$, where $b_{\rm max}$ is the maximum distance at which a devil detectable. Thus, the average miss distance is $\langle b/\Gamma_{\rm act}\rangle = \int b/\Gamma_{\rm act}\ dp = 2/3\ b_{\rm max}/\Gamma_{\rm act} \approx 1/3\sqrt{P_{\rm act}/P_{\rm th}}$, for $P_{\rm act} \gg P_{\rm th}$. For example, if $P_{\rm act} \approx 10\ P_{\rm th}$, $\langle b\rangle \approx \Gamma_{\rm act}$, and so $P_{\rm obs} \approx P_{\rm act}/5$ and $\Gamma_{\rm obs} \approx 5\ \Gamma_{\rm act}$.

As it travels, the pressure contour $P_{\rm th}$ carves out a long, narrow area $A(P_{\rm act}, \Gamma_{\rm act})$. If a barometer lies within that area, the devil will be detected.

$$A \approx (\Gamma_{\rm act}/2)\sqrt{\frac{P_{\rm act} - P_{\rm th}}{P_{\rm th}}}\upsilon L, \tag{3}$$

where L is a devil's lifetime. Thus, the observed population will be skewed toward the widest devils by a factor

$$f = \frac{A(\Gamma_{\rm act}, P_{\rm act})}{A_{\rm max}} = A_{\rm max}^{-1}\ \Gamma_{\rm act}\sqrt{\frac{P_{\rm act} - P_{\rm th}}{P_{\rm th}}}\upsilon\ L, \tag{4}$$

where $A_{\rm max}$ is the area of the very largest devil.

Incorporating this signal distortion and recovery bias, we can convert the underlying distribution of dust devil pressure depths and profile widths $\rho(\rm act)$ to the observed distribution $\rho(\rm obs)$:

$$\rho(\rm obs) = \int f\ \rho(\rm act(\it b'\rm))\ \frac{2b'\ db'}{b_{\rm max}^2}, \tag{5}$$

where the integral is taken over all allowable miss distances.

Figure 3 shows how the distortion and bias skew an underlying distribution uniform in pressure depth and profile width. The uniform distribution is severely skewed toward shallower ($P_{\rm obs}$ small) and wider ($\Gamma_{\rm obs}$ large) profiles.

Conclusions: Relating the population statistics of dust devils to their underlying physical structures relationships is critical for understanding the atmospheric influence of devils on Mars since it depends so sensitively on both the devils' statistical and physical properties. For example, [2] suggested an exponential dependence of dust flux on a dust devil's pressure depth, and using our model to de-bias the survey of Martian devils from [3] suggests a dust flux at least 30% larger than implied by the observed population.

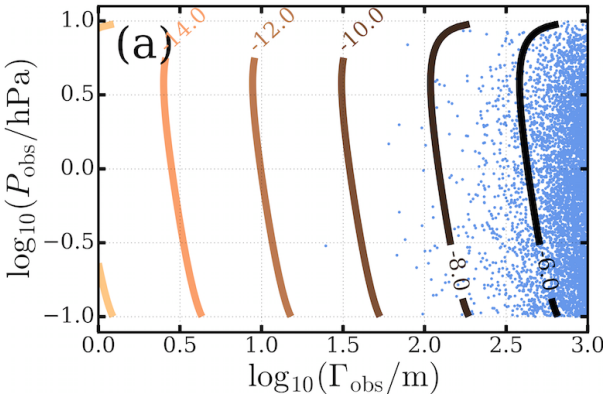

Figure 3: Contours of number density for observed parameters, assuming a uniform distribution of underlying values. The blue circles show a simulated survey.

References

[1] Shabari Basu. Simulation of the Martian dust cycle with the GFDL Mars GCM. *J. Geophys. Res.*, 109(E11), 2004. doi:10.1029/2004je002243.

[2] Lynn D. V. Neakrase, et al. Dust flux within dust devils: Preliminary laboratory simulations. *Geophys. Res. Lett.*, 33(19), 2006. doi:10.1029/2006gl026810.

[3] M. D. Ellehoj, et al. Convective vortices and dust devils at the Phoenix Mars mission landing site. *J. Geophys. Res.*, 115, 2010. doi:10.1029/2009je003413.

[4] Ralph D. Lorenz. Power law distribution of pressure drops in dust devils: Observation techniques and Earth–Mars comparison. *Planetary and Space Science*, 60(1):370–375, 2012. doi:10.1016/j.pss.2011.11.003.

[5] Ralph D. Lorenz. Vortex Encounter Rates with Fixed Barometer Stations: Comparison with Visual Dust Devil Counts and Large-Eddy Simulations. *J. Atmos. Sci.*, 71(12):4461–4472, 2014. doi:10.1175/jas-d-14-0138.1.

[6] Brian Jackson and Ralph Lorenz. A multiyear dust devil vortex survey using an automated search of pressure time series. *J. Geophys. Res. Planets*, 120(3):401–412, 2015. doi:10.1002/2014je004712.